Desalination and Water Treatment
www.deswater.com
doi: 10.1080/19443994.2015.1054313

57 (2016) 12415–12423
June

Taylor & Francis
Taylor & Francis Group

$CaCO_3$ scaling of oilfield produced water in "electrochemical pre-oxidation–coagulation sedimentation–filtration" process: reason, mechanism, and countermeasure

Jian Wang[a,b], Xueli Gao[a,b,*], Zhaokui Li[c], Yuhong Wang[d], Congjie Gao[a,b]

[a]*Ministry of Education, Key Laboratory of Marine Chemistry Theory and Technology, Ocean University of China, Qingdao 266100, China, email: swordking8856@163.com (J. Wang), Tel./Fax: +86 532 66782017; emails: swordking8856@hotmail.com, gxl_ouc@126.com (X. Gao), gaocjie@ouc.edu.cn (C. Gao)*
[b]*College of Chemistry and Chemical Engineering, Ocean University of China, Qingdao 266100, China*
[c]*Institute of Tianjin Seawater Desalination and Multipurpose Utilization, State Oceanic Administration, Tianjin 300192, China, email: lzksoa@126.com*
[d]*National Center of Ocean Standards and Metrology, Tianjin 300112, China, email: wangyuhong@ncosm.gov.cn*

Received 28 August 2014; Accepted 6 May 2015

ABSTRACT

Chemical stability of oilfield injection water is a critical factor to avoid corrosion and scaling of water treatment devices and pipelines. Especially, Guangli oilfield (a branch of Shengli Oilfield) has achieved remarkable success in anti-corrosion by applying an electrochemical pre-oxidation process into strong corrosive wastewater treatment, while scaling was aggravated therefore. XRD, SEM, EDS, and chemical analysis demonstrated the major component of the scale deposit was calcite. Succeedingly, chemical analysis of produced water along the process showed that pH, concentration of calcium ions, bicarbonate ions, and suspended solids changed remarkably before and after the mixing reactor. Further studies revealed that the addition of water treatment chemicals (Na_2CO_3) in the mixing reactors induced the precipitates of $CaCO_3$, which could serve as crystal seeds and resulted in the continuous precipitation of calcium ions. Moreover, calcite saturation ratio increased from 0.97 to 3.94 could contribute to the rise of pH and bicarbonate ions. Consequently, both of them created favorable conditions for crystal growth and incurred more severe scaling problem. The final scale inhibition experiments suggested that the amount of calcium carbonate scale could be mitigated through the dose of scale inhibitors.

Keywords: Produced water treatment; $CaCO_3$ scale; Scaling; Scale inhibitor

1. Introduction

The corrosiveness and scaling of produced water are two important issues in oilfields. The produced water in some areas of Shengli Oilfield, the second largest oilfield in China, possesses high salinity and strongly corrosive property. A targeted electrochemical pre-oxidation process has been effectively used to resolve the corrosion problem. In Guangli Oilfield, the corrosion rate was reduced from 1.6 mm a year to 0.076 mm a year. Unfortunately, severe scaling were observed in several months, and the thickness of the

*Corresponding author.

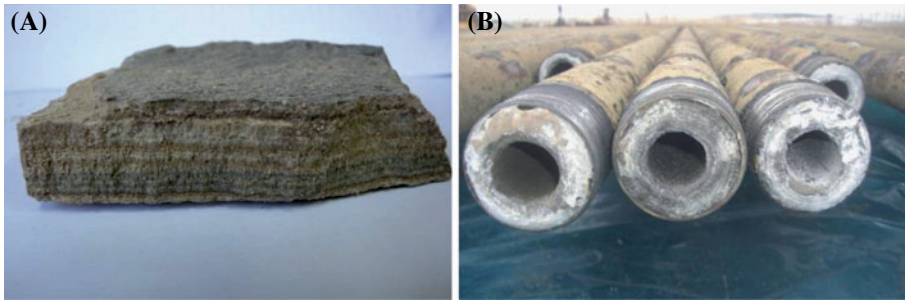

Fig. 1. Pictures of scales formed in produced water treatment plant (A) and injection pipes (B) in Guangli Oilfield.

scale could reach up to 50 mm both in produced water treatment plant (PWTP) and injection wells (as shown in Fig. 1).

Fundamentals of electrochemical pre-oxidation technology could be concluded as electrochemical oxidation/reduction, electrochemical sterilization, and electrochemical coagulation. During this process, Fe^{2+} and S^{2-} could be oxidized into Fe^{3+} and S, respectively, which could be easily removed by the aid of coagulant. In order to obtain better coagulation sedimentation effect in the electrochemical pre-oxidation process, alkaline reagents (such as NaOH and Na_2CO_3) are accustomed to adjusting pH of the wastewater [1]. Meanwhile, alkaline reagents can also be employed to solve corrosion problems by transforming corrosive carbon dioxide into carbonate ions. As carbonate ions could react with calcium ions to form calcium carbonate deposits, the corrosive carbon dioxide will be removed [2,3]. The mechanism can be described as follows [4]:

(1) $CO_2 + H_2O \leftrightarrow H_2CO_3 \leftrightarrow HCO_3^- + H^+ \leftrightarrow CO_3^{2-} + 2H^+$
(2) $OH^- + H^+ \rightarrow H_2O$
(3) $Ca^{2+} + CO_3^{2-} \rightarrow CaCO_3 \downarrow$

pH adjustment for electrochemical pre-oxidation process differs from that for ease of corrosion problems. Electrochemical pre-oxidation process usually set pH in the range of 6.5–7.0 in order to improve coagulation sedimentation effect [2]. However, for the ease of corrosion problems, pH is always controlled around 8.0 to eliminate influencing factors (such as free dioxide and calcium ions) related to corrosion [4]. It is noteworthy that carbonate equilibrium system and calcite saturation ratio would be affected even if the purpose of the pH adjustment is to improve coagulation sedimentation effect. Relatively higher concentration of alkaline reagents can easily lead to the precipitate of calcium carbonate, especially during the mixing course between wastewater and chemical reagents. What's more, the calcium carbonate precipitate may serve as crystal seed and lead to more severe scaling problem. Additionally, many researchers have pointed out that the formation of calcium carbonate scale could be affected by changing of pH values [5–11], pressure [12], temperature [13], and salinity [14,15], etc.

An investigation of the scaling potential in different sites of the oilfield produced water treatment process revealed that the most severe scale phenomenon occurred between the mixing reactors and the buffer tanks. Acid-soluble test indicated that the main component of the scale was carbonate, which mainly refers to calcium carbonate. According to the above analysis, we propose that the water treatment chemicals, which were added in mixing reactors to improve coagulation sedimentation effect, were the culprit of scaling. In this study, detailed investigation was undertaken to corroborate the hypotheses. The scale between the mixing reactors and buffer tanks in the water treatment plant, and the water quality along the process was analyzed. Factors which induce scaling were studied and the scaling mechanism was proposed. Additionally, a preliminary anti-scaling experiment was carried out to evaluate the efficiency of scale inhibitors.

2. Materials and methods

2.1. Process of the produced water treatment plant (PWTP)

Schematic diagram of the Guangli Oilfield produced water treatment process is illustrated in Fig. 2. Produced water was first treated by the electrochemical pre-oxidation devices to remove unstable ions, such as Fe^{2+}, S^{2-}, and free carbon dioxide, followed by removing of oil in the de-oil tanks. After that, it flowed through mixing reactors with dosage of chemical reagents (including coagulant, alkaline reagents, etc.)

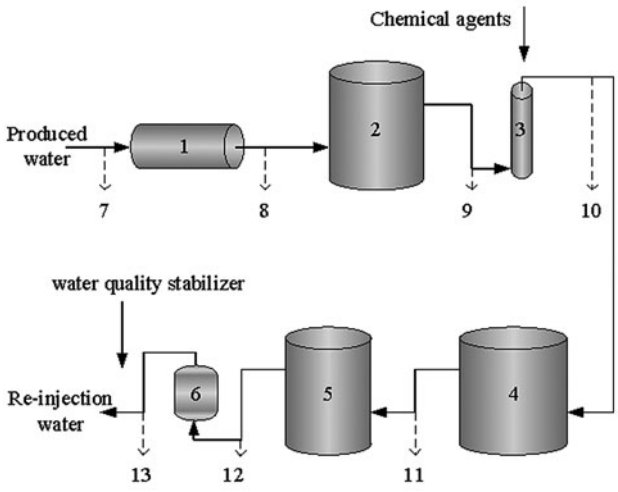

Fig. 2. Schematic diagram of the flowchart of "Electrochemical pre-oxidation + Coagulation sedimentation + Filtration" process in Guangli oilfield. 1—electrochemical pre-oxidation device, 2—de-oil tanks, 3—mixing reactors, 4—settling tanks, 5—buffer tanks, 6—sand filters; 7–13: sampling points.

in order to promote the precipitation of suspended solid (SS) in settling tanks. After that, the water is stored in buffer tanks and further treated by sand filters before sending it back to the injection station.

2.2. Analysis of the scale

Two scale samples were taken from location 10 and 11, respectively. Calcium and magnesium contained in the scale was determined by EDTA titration method [16]. And the content of calcium carbonate (MF) in the scale was calculated as following:

$$\mathrm{MF} = \frac{c(\mathrm{Ca}^{2+}) \cdot V \cdot M}{m} \times 100\% \quad (1)$$

where MF—mass fraction of calcium carbonate in the scale, %; m—weight of the scale sample, g; V—volume of the dissolved scale sample solution, L; $c(\mathrm{Ca}^{2+})$—concentration of calcium ions in the dissolved solution, mol L^{-1}; M—the molecular weight of calcium carbonate, g mol^{-1}.

The micromorphology of the scale was examined using a scanning electron microscopy (SEM S-4800) equipped with X-ray energy dispersion (EDS), which allows the qualitative and quantitative elemental analysis.

The crystal form of calcium carbonate contained in the scale was determined by X-ray diffractometer (Bruker D8 Advance, Germany).

2.3. Water quality analysis

Produced water from sampling points 7 to 13 were collected in order and the interval time was the same as the hydraulic retention time of the corresponding unit. Water sampling and analysis method referred to SY/T0600 [16]. SS, temperature, and pH were measured by the gravimetric method, thermometer, and acidity meter, respectively. Cations including Ba^{2+}, Sr^{2+}, Na^{+}, K^{+}, and anions including SO_4^{2-} and Cl^{-} were measured with ion chromatography (Dionex ICS-90, USA).

The scale samples were dissolved in hydrochloric acid and diluted with de-ionic water. Thereafter, Ca^{2+} and Mg^{2+} were determined by EDTA titration method. CO_3^{2-} and HCO_3^{-} were determined by the potentiometric titration method.

2.4. Scaling tendency analysis

2.4.1. Calcite saturation ratio (CSR)

CSR was calculated to characterize the scaling tendency of the treated water [17]:

$$\mathrm{CSR} = \frac{c(\mathrm{Ca}^{2+}) \cdot \gamma(\mathrm{Ca}^{2+}) \times c(\mathrm{CO}_3^{2-}) \cdot \gamma(\mathrm{CO}_3^{2-})}{K_{\mathrm{sp,CaCO_3}}} \quad (2)$$

where $c(\mathrm{Ca}^{2+})$—the concentration of calcium ions, mol L^{-1}; $\gamma(i)$—activity coefficient of species i ions calculated by Debge–Hückel formula [18]; $K_{\mathrm{sp,CaCO_3}}$—solubility product of $CaCO_3$, 1.759×10^{-9} at 333.15 K [19]; $c(\mathrm{CO}_3^{2-})$—the concentration of carbonate ions (mol L^{-1}), which could be calculated by the following equation according to carbonate equilibrium:

$$c(\mathrm{CO}_3^{2-}) = \frac{c(\mathrm{HCO}_3^{-}) \cdot \mathrm{K}_2}{c(\mathrm{H}^{+})} \quad (3)$$

The ionization constant of bicarbonate ions (K_2) was calculated by [20]:

$$pK_2 = \frac{290239}{T} + 0.02379 \cdot T - 6.498 \quad (4)$$

where T—temperature, K.

2.4.2. Determine the loss of calcium ions

Produced water samples were collected as the method described in Section 2.3, and then the samples were standing at 313.15 K for 9 h. After filtered with ashless filter paper, the concentrations of calcium ions in the samples were measured by EDTA titration method.

2.5. Measurement of the efficiency of scale inhibitors

Two types of commercial scale inhibitors, named amino trimethylene phosphonic acid (inhibitor A) and 1-hydroxy ethylidene-1,1-diphosphonic acid (inhibitor B), that are widely used in oilfields were added into the produced water of sampling point 11 with different concentration (2, 5, 10, 15, 20, and 30 mg L^{-1}). Next, the mixtures were standing at 333.15 K. After 9 h, the concentration of calcium ions was measured. Efficiency of scale inhibitors (I) was calculated as follows:

$$I(\%) = \frac{c_2 - c_1}{c_0 - c_1} \times 100\% \quad (5)$$

where c_0—calcium ions concentration in raw produced water samples, mol L^{-1}; c_1—calcium ions concentration in produced water samples without scale inhibitors and treated by set statically at 333.15 K for 9 h, mol L^{-1}; c_2—calcium ions concentration in produced water samples with scale inhibitors and treated by set statically at 333.15 K for 9 h, mol L^{-1}.

3. Results and discussion

3.1. Analysis of the scale

The amount of calcium and magnesium in the scale was shown in Table 1. The result indicated that the main composition of the scale was $CaCO_3$ which accounted for about 83% in mass fraction, while the amount of magnesium in the scale was relatively lower. The EDS results were shown in Fig. 3, it could be seen that the main elements in the scale including calcium, magnesium, carbon, and oxygen which also meant that the main composition of the scale was $CaCO_3$.

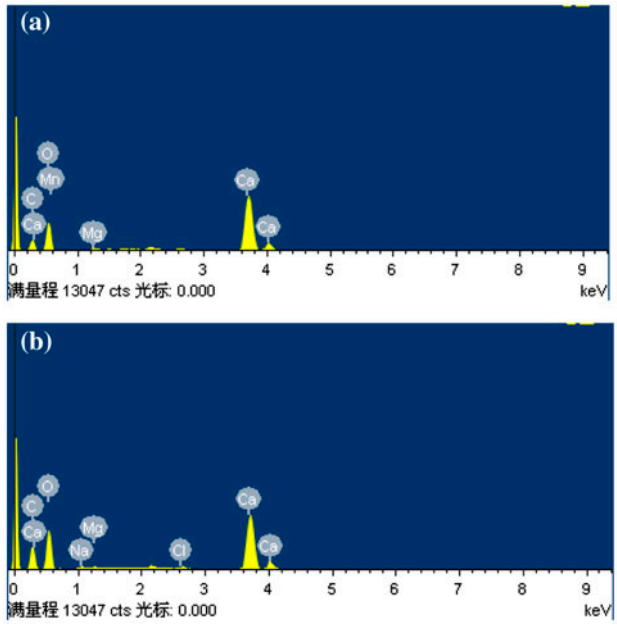

Fig. 3. EDS results of the scales from (a) sampling point 10 and (b) sampling point 11.

Scale samples were also subjected to SEM analysis. As shown in Fig. 4, the micromorphology of the scales tended to form rhombic crystal instead of needle-like crystal or spherical crystal. A lot of literature [13,17,18,21] had described the micromorphology of $CaCO_3$. Calcite and aragonite usually crystallized as monocrystalline well-faceted particles (rhombohedral for calcite and needle-like for aragonite crystals), while vaterite was poly-crystalline and exhibited a spherical shape [13]. Hence, according to Fig. 4, we suggested that the main crystal-type of the scale in this study was calcite. Further study of the scale was performed with XRD, as shown in Fig. 5. The results indicated that the dominant crystal-type was calcite, 2θ = 23.14, 29.51, 36.09, 39.55, 43.31, 47.27, 47.71, 48.70, 56.80, 57.60, and small amount of aragonite was also

Table 1
Results of chemical analysis of scale

	Mass fraction (%)		
Sampling point	Calcium	Magnesium	Calcium carbonate
10	33.3	2.48	83.1
11	33.8	2.73	84.4

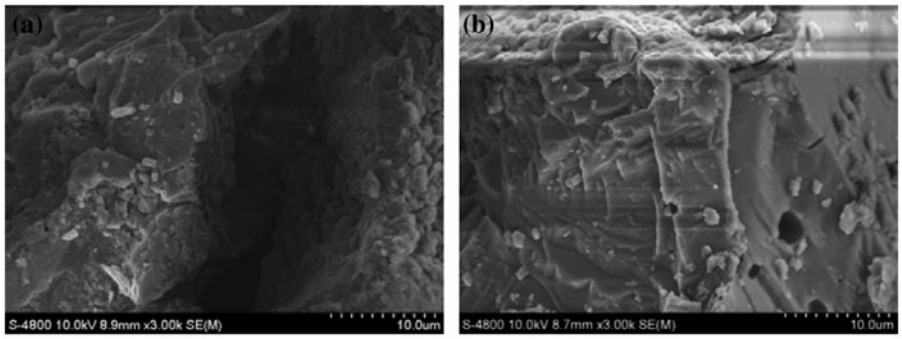

Fig. 4. Micromorphology of scales from (a) location 10 and (b) location 11.

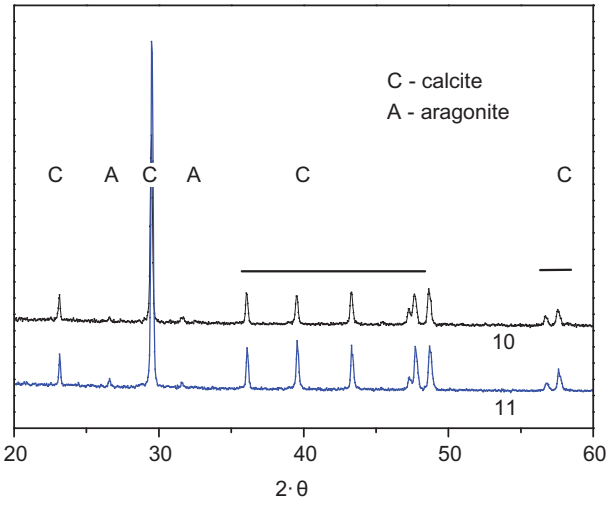

Fig. 5. XRD curves of $CaCO_3$ species from location 10 and location 11.

detected at $2\theta = 26.59, 31.69$. Similar results also could be seen elsewhere [12,22]. Therefore, the conclusion can be drawn that the main composition of the scale was $CaCO_3$, of which the dominant crystal-type is calcite.

According to Gal et al. [8] and Sawada [23], calcite was the most stable form with a solubility product of $10^{-8.48}$ at 298.15 K and widely exists in nature; aragonite is a less stable form with a solubility product of $10^{-8.34}$ at 298.15 K and mainly biosynthetic; vaterite is the most unstable form with a solubility product of $10^{-7.91}$ at 298.15 K and rarely occurs in nature, but it always precipitated initially from the supersaturated solution and plays an important role in the precipitation of calcium carbonate [23].

As there is barely scale formed before mixing reactors in the PWTP, we suggested that the $CaCO_3$ scale formed in this study might be transformed from vaterite.

3.2. Water analysis

Results of the chemical analysis of the produced water were represented in Table 2. Along the treatment process, the temperatures and the concentrations of sodium, potassium, magnesium, and chloride ions

Table 2
Water quality results along the process

Sampling points	7	8	9	10	11	12	13
Temperature (℃)	58.8	59.2	58.8	58.8	58.6	58.2	58.2
pH	6.51	6.41	6.43	6.98	6.82	6.84	6.86
SS (mg L^{-1})	11.3	42.0	47.0	69.0	20.4	23.2	1.0
Na^+ (mg L^{-1})	13,521	13,521	13,525	13,524	13,517	13,520	13,515
K^+ (mg L^{-1})	229	229	222	227	223	225	219
Ca^{2+} (mg L^{-1})	1737	1736	1735	1728	1723	1719	1719
Mg^{2+} (mg L^{-1})	314	315	314	313	313	313	313
Cl^- (mg L^{-1})	24,854	24,837	24,840	24,833	24,842	24,839	24,833
HCO_3^- (mg L^{-1})	384	366	363	417	409	402	396
TDS (mg L^{-1})	41,044	41,008	41,005	41,046	41,032	41,024	40,999

Note: Ba^{2+}, Sr^{2+} and SO_4^{2-} were not detected.

were relatively stable. However, the values of SS, pH, and concentrations of calcium ions and bicarbonate ions varied drastically. The amount of SS, as shown in Table 2, increased sharply after the electrochemical pre-oxidation process. And the addition of alkaline agent (Na_2CO_3) in mixing reactors resulted in the sharp increase in pH and concentration of bicarbonate ions. At the same time, as can be seen from the sample point 10 of Table 2, calcium carbonate was precipitated and led to the substantially increase in SSs. After that, the amount of calcium ions decreased gradually along the process because the calcium carbonate deposit acts as crystal seeds, as well as the increased pH and concentration of bicarbonate ions. These results indicated that the main component of the scale was calcium carbonate.

Many researchers had also pointed out that pH value [6,7,11], alkalinity or concentration of crystal seed [14], and bicarbonate ions [14,15] played an important role in the precipitation of $CaCO_3$. Therefore, we had proved that the water treatment chemicals were the culprit of the precipitation of $CaCO_3$.

3.3. Scaling tendency analysis

Temperature was set at 333.15 K to facilitate the calculation. The CSR calculated according to Eq. (2) was shown in Table 3.

The results showed that calcium carbonate in the produced water was hardly supersaturated before the mixing reactors (location 9 in Table 3), with SCR around 1.0. But after that, CSR value increased sharply up to 3.94, which implied more severe scaling tendency. Even CSR value decreased along the process after mixing reactors, it is still above 2.5. The CSR tendency had been demonstrated by the PWTP practice, in which the scaling tendency between the mixing reactors and the settling tanks, where the CSR value was the highest, was most serious.

However, the increasing trend of CSR value was in contrary to the observations that scaling phenomenon was gradually reduced after the settling tanks. Gal et al. [8] and Yin et al. [24] had pointed out that only the high CSR was not enough to induce more severe scaling problem. Therefore, the degree of supersaturation of calcium carbonate in produced water was not the sole cause of $CaCO_3$ precipitation.

The results of the loss of calcium ions along the treatment process were shown in Fig. 6. The loss of calcium ions was less than 8 mg L^{-1} before location 10, while it was up to 23 mg L^{-1} after location 9. Thereafter, loss of calcium ions decreased along the process, which was in contrary to the variation trend of CSR value. These results demonstrated that, as discussed previously, the degree of supersaturation of calcium carbonate in produced water after location 9 was not the sole cause of $CaCO_3$ precipitation. We proposed that, according to the water analysis results shown in Table 2, variation of SS would be another factor.

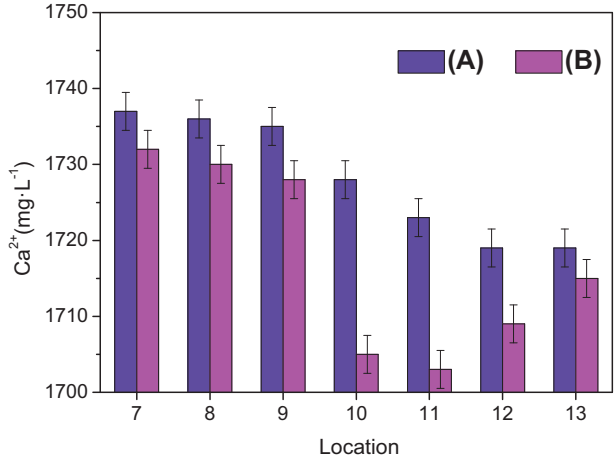

Fig. 6. Scaling tendency of produced water at different sampling point of the water treatment process (concentration of calcium ions in (A) raw samples and (B) samples that standing for 9 h).

Table 3
Results of water analysis along the process

Location	7	8	9	10	11	12	13
K_2	7.25×10^{-11}						
$\gamma(Ca^{2+})$	0.202						
$\gamma(CO_3^{2-})$	0.167						
$Ca(\times 10^{-2}$ mol $L^{-1})$	4.34	4.34	4.34	4.32	4.31	4.30	4.30
$CO_3^{2-}(\times 10^{-6}$ mol $L^{-1})$	1.26	1.12	1.16	4.73	3.52	3.38	3.18
CSR	1.05	0.93	0.97	3.94	2.66	2.73	2.82

3.4. Study on key influencing factors

In order to investigate the influence of SS, pH, and concentration of bicarbonate ions on calcium carbonate precipitation, produced water samples from location 9, 10, and 11 were taken and, immediately, the concentration of calcium ions was measured. Each of the samples was divided into two parts: one part was filtered with ashless filter paper to eliminate the effect of SS on the precipitation of calcium carbonate; and the other part that without any treatment was marked as raw sample. And then the samples were tackled according to Section 2.4.2.

The results of the effect of pH, SSs, and concentration of bicarbonate ions on $CaCO_3$ precipitation were presented in Fig. 7. Concentration of calcium ions in the filtered samples from location 9, 10, and 11 were approximately equal to that of the raw samples. However, concentration of calcium ions in the raw samples was reduced obviously. That meant the variation of pH and concentration of bicarbonate ions, as shown in Table 2, had little effect on the precipitation of calcium carbonate. The raw sample from location 9 had a very lower loss amount of calcium ions while the raw samples from location 10 and 11 had a relatively higher loss amount of calcium ions, 23 and 20 ppm, respectively. Therefore, it could be concluded that the SS, when compared with that of pH and concentration of bicarbonate ions, was the key factor in the precipitation of calcium ions.

Crystal growth theory suggested that calcium carbonate scaling included two steps—nuclei formation and crystal growth, and both of them were key factors in crystal precipitation [25]. Crystal nucleus, under normal circumstances, was not necessarily produced even at high degree of supersaturation when the liquid phase was under thermodynamically stable state. But once the stable state was broken, crystal nucleus would be formed and then growing until another thermodynamically stable state was created. In this study, water treatment reagents added in the mixing reactors broke the thermodynamically stable state and caused the precipitation of $CaCO_3$, which resulted in the increase in the content of SS. In Fig. 7, as the SS in the filtered samples was removed, the growth rate of calcium carbonate was almost zero because the $CaCO_3$ precipitation from water under the existence of crystal seed was surface reaction controlled [26,27].

What's more, the deposition rate of calcium carbonate was accelerated by the correspondingly increased CSR. Xing et al. [9] indicated that scaling tendency of calcium carbonate increasing linearly with the increase in pH when it was lower than 8.0. Zhang and Dawe [14] pointed out that the reaction order of calcium carbonate precipitation increasing with the increase in pH, when it was lower than 7.0. Therefore, the degree of supersaturation of calcium carbonate would certainly impact on the deposition rate of calcium carbonate.

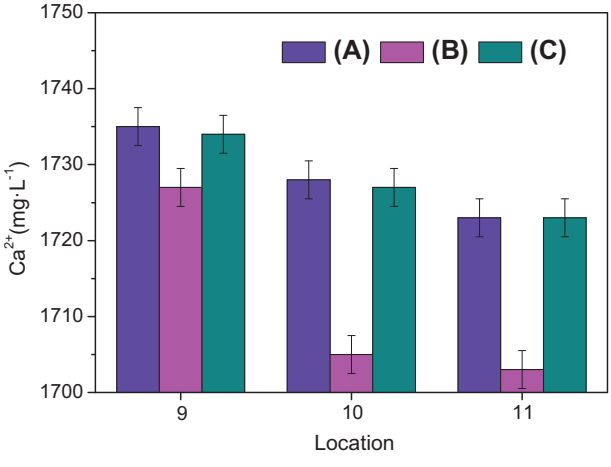

Fig. 7. Concentration of calcium ions in (A) raw samples, (B) raw samples that standing for 9 h and (C) filtered samples that standing for 9 h at sampling points of 9, 10 and 11.

3.5. Scaling mechanisms and efficiency of scale inhibitors

According to the above analysis, the increase in pH value (from 6.43 to 6.98) led to the right shift of the carbonate equilibrium system, which was showed in the reaction formula (1). This further resulted in the increase in CSR (from 0.97 to 3.94). Both of calcium carbonate precipitation and high CSR contributed to the severe scaling phenomena between the mixing reactors and buffer tanks. Mechanisms of calcium carbonate precipitation could be deduced as follows:

$$(4)\quad CO_3^{2-} + Ca^{2+} = CaCO_3 \downarrow$$
$$(5)\quad H_2CO_3 + OH^- = HCO_3^- + H_2O$$
$$(6)\quad 2HCO_3^- + Ca^{2+} = CaCO_3 \downarrow + H_2O + CO_2$$

Chemical Eqs. (4) and (6) indicate the formation of crystal seed and growing of calcium carbonate, respectively. Chemical Eq. (5) referred to the increase in pH and concentration of bicarbonate ions caused by adding an alkaline agent.

Scale inhibitors were often used to inhibit scale formation in oilfields. Two types of commercial scale inhibitors widely used in oilfields were chosen to investigate their inhibiting efficiency. According to Section 2.5, the results were represented in Fig. 8. The

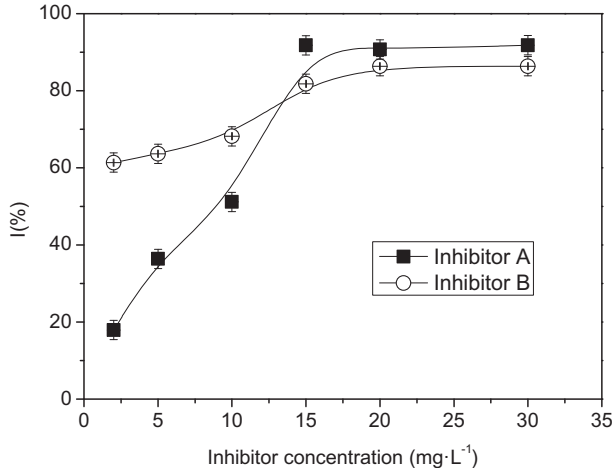

Fig. 8. Efficiency of scale inhibitors on produced water sampling at location 11.

results indicated that the efficiency of inhibitor A was increased from 18 to 92% for calcium ions as the concentration of inhibitor increased from 2 mg L^{-1} to 30 mg L^{-1}. Whereas the efficiency of inhibitor B did not significantly increases as the concentration of inhibitor increased. These results indicated that the optimum dosage of both inhibitors should not be less than 15 mg L^{-1}. Just considering the efficiency of both inhibitors, inhibitor A, of which the efficiency is above 90% when the concentration is higher than 15 mg L^{-1}, is superior to inhibitor B.

4. Conclusion

(1) The scaling problem in Guangli Oilfield was attributed to water treatment chemicals added in mixing reactors.
(2) The main composition of the scale in the Guangli PWTP and the injection well was carbonate (mainly calcite), of which the mass fraction was more than 80%.
(3) The formation of $CaCO_3$ deposit combine with the high CSR resulted in the severe scaling between the mixing reactors and the buffer tanks.
(4) Precipitation of calcium carbonate could be inhibited by adding scale inhibitors with a dosage that higher than 15 mg L^{-1}.

Acknowledgments

This work was financially supported by the foundation of the High Science and Technology Project of China (No.2012AA03A602), Shandong Major Project of Science and Technology (2012CX7301), and Public Science and Technology Research Funds Projects of Ocean (201305039). The authors would like to thank Guangli Oilfield Produced Water Treatment Plant.

Nomenclature

MF	—	mass fraction of calcium carbonate in the scale (%)
$c(i)$	—	concentration of species i (mol L^{-1})
V	—	volume of the dissolved scale sample solution (L)
M	—	the molecular weight of calcium carbonate (g mol^{-1})
m	—	weight of the scale sample (g)
CRS	—	calcite saturation ratio in produced water samples
$\gamma(i)$	—	activity coefficient of species i
$K_{sp,CaCO_3}$	—	solubility product of $CaCO_3$, which is 1.759×10^{-9} at 333.15 K
T	—	temperature (K)
K_2	—	ionization constant of bicarbonate ions
I	—	efficiency of scale inhibitors (%)
c_i	—	concentration of calcium ions (mol L^{-1})

References

[1] G. You, G. Liu, T. Zhou, Y. Xiao, Y. Cao, Application of electrochemistry pre-oxidation technology to the treatment of effluent at Shinan Station, Ind. Water Treat. 26 (2006) 90–92.
[2] D. Wang, M. Huang, F. Li, L. Luo, X. Zhang, Studies on improving quality of recycled produced water of Guangli Water Treating Plant for reservoir flooding, Oilfield Chem. 21 (2004) 154–159.
[3] Y. Ji, A. Zhang, L. Zhang, S. Fu, Injection water quality adjustment for reservoir flooding at Zhongyuan oil fields, Oilfield Chem. 20 (2003) 13–16.
[4] Y. Chen, F. Fan, H. Cong, Quality Adjustment Technology for Oilfield Produced Water, China University of Petroleum Press, Dongying, 2006.
[5] S.A. Parsons, B. Wang, S.J. Judd, T. Stephenson, Magnetic treatment of calcium carbonate scale-effect of pH, Water Res. 31 (1997) 339–342.
[6] I.S. Al-Mutaz, M.A. Al-Ghunaimi, pH control in water treatment plant by the addition of carbon dioxide, in: The IDA World Congress on Desalination and Water Reuse, Bahrain, 2001, pp. 1–12.
[7] T. Østvold, P. Randhol, Kinetics of $CaCO_3$ scale formation—The influence of temperature, supersaturation and ionic composition, in: International Symposium on Oilfield Scale, Society of Petroleum Engineers Aberdeen, United Kingdom, 2001, pp. 1–9.
[8] J.-Y. Gal, Y. Fovet, N. Gache, Mechanisms of scale formation and carbon dioxide partial pressure influence. Part I. Elaboration of an experimental method and a scaling model, Water Res. 36 (2002) 755–763.

[9] X. Xing, C. Ma, Y. Chen, An experimental study of influence of pH on calcium carbonate crystallization fouling, Petro-Chem. Eq. 33 (2004) 11–15.
[10] S. Baraka-Lokmane, K.S. Sorbie, Effect of pH and scale inhibitor concentration on phosphonate–carbonate interaction, J. Petrol. Sci. Eng. 70 (2010) 10–27.
[11] Y.F. Ma, Y.H. Gao, Q.L. Feng, Effects of pH and temperature on $CaCO_3$ crystallization in aqueous solution with water soluble matrix of pearls, J. Cryst. Growth 312 (2010) 3165–3170.
[12] K.A. Kodel, P.F. Andrade, J.V.B. Valença, D.d.N. Souza, Study on the composition of mineral scales in oil wells, J. Petrol. Sci. Eng. 81 (2012) 1–6.
[13] C. Martos, B. Coto, J.L. Pen, R.R. Guez, D. Merino-Garcia, G. Pastor, Effect of precipitation procedure and detection technique on particle size distribution of $CaCO_3$, J. Cryst. Growth 312 (2010) 2756–2763.
[14] Y. Zhang, R. Dawe, The kinetics of calcite precipitation from a high salinity water, Appl. Geochem. 13 (1998) 177–184.
[15] S. Jiang, H. Yu, C. Liu, Research on the scaling dynamic model of the high salinity system, Appl. Chem. Ind. 40 (2011) 1623–1629.
[16] SY/T0600, Predication of scaling tendency in oilfield water, in: Predication of Scaling Tendency in Oil-Field Water, National Energy Administration, Beijing, 1997.
[17] R.A. Dawe, Y. Zhang, Kinetics of calcium carbonate scaling using observations from glass micromodels, J. Petrol. Sci. Eng. 18 (1997) 179–197.
[18] Z. Nan, Z. Shi, B. Yan, R. Guo, W. Hou, A novel morphology of aragonite and an abnormal polymorph transformation from calcite to aragonite with PAM and CTAB as additives, J. Colloid Interface Sci. 317 (2008) 77–82.
[19] SequentiX Software, Calculation of ion activity products and the calcite saturation index, 2011.
[20] R.N. Roy, L.N. Roy, K.M. Vogel, C. Porter-Moore, T. Pearson, C.E. Good, F.J. Millero, D.M. Campbell, The dissociation constants of carbonic acid in seawater at salinities 5 to 45 and temperatures 0 to 45 ℃, Mar. Chem. 44 (1993) 249–267.
[21] J. Świetlik, U. Raczyk-Stanisławiak, P. Piszora, J. Nawrocki, Reasons for the lack of chemical stability of treated water rich in magnesium, Water Res. 45 (2011) 6585–6592.
[22] R. Ketrane, L. Leleyter, F. Baraud, M. Jeannin, O. Gil, B. Saidani, Characterization of natural scale deposits formed in southern Algeria groundwater: Effect of its major ions on calcium carbonate precipitation, Desalination 262 (2010) 21–30.
[23] K. Sawada, The mechanisms of crystallization and transformation of calcium carbonates, Pure Appl. Chem. 65 (1997) 921–928.
[24] X. Yin, J. Wu, Z. Wang, Analysis and prediction of scaling mechanism of the $CaCO_3$ from oilfield injection waters, Petrol. Explor. Dev. 29 (2002) 85–87.
[25] W.Q. Jie, Principle and Technology of Crystal Growth, Science Press, Beijing, 2010.
[26] M.M. Reddy, G.H. Nancollas, The crystallization of calcium carbonate: I. Isotopic exchange and kinetics, J. Colloid. Interface Sci. 36 (1971) 166–172.
[27] M.M. Reddy, W.D. Galliard, Kinetics of calcium carbonate (calcite)-seeded crystallisation: Influence of solid/solution ratio on the reaction rate constant, J. Colloid. Interface Sci. 80 (1981) 171–178.